The first unpaired electron placed inside a C_3-symmetry P-chirogenic cluster†

Christine Salomon,[a,b] Sophie Dal Molin,[b] Daniel Fortin,[a] Yves Mugnier,[b] René T. Boeré,[c] Sylvain Jugé*[b] and Pierre D. Harvey*[a]

Received 25th May 2010, Accepted 4th June 2010
DOI: 10.1039/c0dt00542h

The $Pd_3(dppm^*)_3(CO)^{n+}$ enantiomers ($n = 2$ (**2**), 1 (**3**)) were prepared either from (*R*,*R*)- or (*S*,*S*)-*P*-chirogenic bis(phenyl-*m*-xylylphosphino)methane (dppm*; **1**) and $Pd(OAc)_2$ in the presence of CF_3CO_2H, CO and water ($n = 2$), and then by reductive electrolysis ($n = 1$). The stable enantiomeric $[Pd_3((S,S)\text{-dppm}^*)_3(CO)]^{+\bullet}$ (**3**), is the first C_3-symmetry radical-cation M-M bonded cluster, therefore the odd electron is delocalized onto the Pd_3 frame within this symmetry. The novel chiral species have been characterized by circular dichroism (CD) of both enantiomers of the $Pd_3(dppm^*)_3(CO)^{2+}$ clusters (**2**) and by EPR spectroscopy for the $Pd_3((S,S)\text{-dppm}^*)_3(CO)^{+\bullet}$ paramagnetic compounds (**3**, $g = 2.041$). Evidence for reduced symmetry with respect to the achiral cluster was also obvious from the hyperfine splittings of the EPR signal which display three different hyperfine coupling values: $3 \times A(^{31}P) = 83.9 \times 10^{-4}$ cm^{-1}, $3 \times A(^{31}P) = 69.7 \times 10^{-4}$ cm^{-1}, $3 \times A(^{105}Pd) = 12.5 \times 10^{-4}$ cm^{-1}. In the absence of an X-ray structure for the paramagnetic clusters, DFT computations were performed to address the geometry. The optimized geometry of the $Pd_3((S,S)\text{-dppm}^*)_3(CO)^{+\bullet}$ radicals (**3**) exhibits three phosphorus atoms placed well above the Pd_3 plane, while the three others are located below the trimetallic frame within C_3-symmetry due to intramolecular steric hindrance. This makes them chemically different with respect to the carbonyl group and explains the experimental EPR spectrum well. Consequently this C_3-symmetry deformation also induces a change in the shape of the SOMO (semi-occupied molecular orbital) towards this same symmetry compared to the corresponding achiral C_{3v} species.

Introduction

Chiral paramagnetic transition metal complexes are numerous and have attracted attention for their potential applications as metalloenzyme models, single-molecule magnets, catalysts and nanoelectronic components.[1–6] On the other hand, chiral paramagnetic binuclear complexes[2] and both M-M bonded and non-M-M-bonded metal clusters[3,4] are scarce and have been generated by redox[5] or electrochemical methods.[6] We recently reported thermal and electrochemical preparation of the first confidently characterized paramagnetic palladium cluster, $[Pd_3(dppm)_3(CO)]^{+\bullet}$ (**3'**, $Pd_3^{+\bullet}$; dppm = $(Ph_2P)_2CH_2$; Scheme 1).[7,8] This species exhibits an unpaired electron delocalized over the three Pd atoms due to Pd–Pd bonding, hence retaining full C_{3v} symmetry. Because of its unsaturated face, this cluster undergoes dismutation to $[Pd_3(dppm)_3(CO)]^{\circ}$ (**4'**) and $[Pd_3(dppm)_3(CO)]^{2+}$ (**2'**) within an hour in solution. Its stability was improved by reversibly protecting it with a capping RC≡CR ligand. However, the formation of such adducts leads to the loss of C_{3v} symmetry as indicated for the diamagnetic dications by three pairs of chemically inequivalent ^{31}P nuclei (AA'BB'XX' system) and in the radical cations by six different phosphorus hyperfine coupling constants.[9,10]

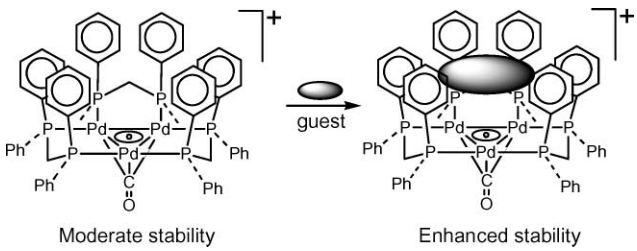

Scheme 1

The first C_3-symmetry P-chirogenic $[Pd_3(dppm^*)_3(CO)]^{2+}$ clusters in which the modified dppm* ligands bear *o*-anisyl and phenyl substituents at each P-centre were just reported by us.[11] This arrangement did not affect the cavity size above the Pd_3 center as the orientation of the OMe groups minimized intramolecular steric hindrance and thus do not provide stability to the corresponding radical cation. Conversely, changing all four phenyl groups of dppm by *m*-xylyl groups would, on the basis of computer modeling, completely obscure the open $Pd_3^{+\bullet}$ face and, while improving its lifetime, would also prevent any substrate from interacting with the very reactive $Pd_3^{+\bullet}$ center. Hence, we elected to substitute two of the four phenyl groups per ligand by *m*-xylyls

[a]*Département de Chimie, Université de Sherbrooke, Sherbrooke, J1K 2R1, Québec, Canada. E-mail: Pierre.Harvey@USherbrooke.ca; Fax: 1-819-821-8017; Tel: 1-819-821-7092*
[b]*Institut de Chimie Moléculaire de l'Université de Bourgogne (ICMUB) UMR CNRS 5260, Université de Bourgogne, 9 avenue Alain Savary, BP 47870, 21078 Dijon Cedex, France. E-mail: Sylvain.Juge@u-bourgogne.fr; Fax: (+33) (0)3 80 39 61 17; Tel: (+33) (0)3 80 39 61 13*
[c]*Department of Chemistry and Biochemistry, University of Lethbridge, Lethbridge, T1K 3M4, Alberta, Canada. E-mail: boere@uleth.ca*
† Contribution from the Université de Sherbrooke, Sherbrooke, PQ, Canada, the Institut de Chimie Moléculaire de l'Université de Bourgogne, Université de Bourgogne, France, and the University of Lethbridge, Lethbridge, Alberta, Canada.

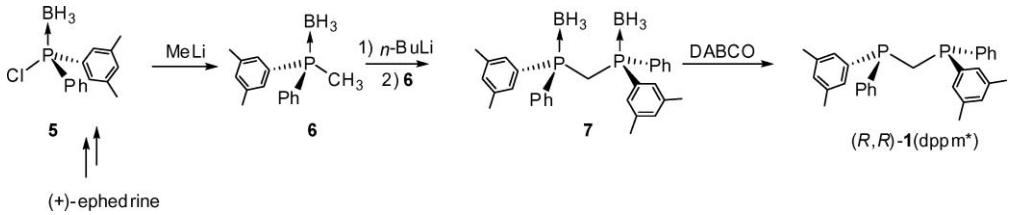

Scheme 2

in a C_2-chiral fashion, so that the cavity would still be symmetric and hopefully be stabilized while remaining accessible.

We now wish to report the synthesis and characterization of $Pd_3(dppm^*)_3(CO)^{n+}$ clusters (dppm* = (*R*,*R*)- and (*S*,*S*)-(*m*-XylPhP)$_2$CH$_2$; $n = 2$ (**2**), 1 (**3**)). The paramagnetic cluster (**2**) is the first example where the odd electron is retained in a C_3-symmetry cluster environment. The recently reported $[Cu_3(\mu^3\text{-}OH)_2]^{4+}$ cluster placed inside a tritopic nonaazapyridinophane macrocycle,[3] exhibits a general molecular structure of C_3-symmetry with three Cu(II) d^9 centers lacking Cu–Cu bonds, so that the odd electrons are not delocalized over the whole structure. Consequently, those unpaired electrons are not placed in a truly C_3-symmetry environment. In addition, the electrochemically generated paramagnetic species $[(\mu_3\text{-}S)Co_3(CO)_7(\mu\text{-}1,3\text{-}\eta^2\text{-}NHC(Me)S]^{\bullet-}$ does not belong to the C_3-symmetry point group.[6]

Results and discussion

The stereoselective synthesis of the (*R*,*R*)- and the (*S*,*S*)-ligands **1** was performed in several steps using the ephedrine methodology and (+)- or (–)-ephedine respectively.[12,13] The key step of the synthesis is the methano bridge formation by reaction of the carbanion derived the methyl phosphine borane **6**, with the chloro phosphine borane **5** (Scheme 2, only the (*R*,*R*)-version is shown).[12,13]

Thus, the reaction of the (*S*)-chlorophenyl-*m*-xylylphosphine borane **5** with the MeLi reagent affords the corresponding (*R*)-methylphosphine borane **6** with inversion of configuration at the P-centre. After deprotonation of the methylphosphine borane **6** with *n*-BuLi, reaction with the (*S*)-chloro phosphine borane **5** afforded the protected diphosphine diborane **7** in good yields (80%). The enantiomeric purity was checked by chiral HPLC using racemic samples of **7** and the *meso*-isomer. The desired free ligand **1** was obtained cleanly after decomplexation of the diborane complex **7** with DABCO (Scheme 2).

The chiral Pd_3^{2+} clusters **2** were prepared using a methodology similar to that outlined by Lloyd and Puddephatt,[14–16] by reacting the (*R*,*R*)- or (*S*,*S*)-(*m*-XylPhP)$_2$CH$_2$ ligands **1** with $Pd(OAc)_2$ in the presence of CF_3CO_2H, CO and water (Scheme 3, only the (*R*,*R*)-version is shown). The relative size of the cavity above the unsaturated Pd_3^{2+} frame was addressed by space-filling computer modelling for various dppm* conformations with respect to the $Pd_3(CO)$ framework in comparison with the achiral version (**2′**)[17] (Fig. 1). The conclusion is that the cavity size is reduced slightly but can accommodate the $CF_3CO_2^-$ ion inside it. This is corroborated by electrochemical findings discussed below.

Evidence for chirality at the Pd_3 center is provided by circular dichroism spectroscopy (CD; Fig. 2, Table 1) where positive and negative signals are observed in the 500-nm region; one known

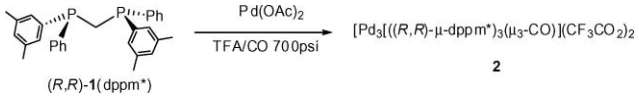

Scheme 3

Table 1 CD data for **2** in THF at 298 K. dppm* = (*R*,*R*)- and (*S*,*S*)-(*m*-XylPhP)$_2$CH$_2$ (**1**)

(*R*,*R*)	λ max (nm)	289	452	529
	θ (mdeg)	4.35	1.1	–0.8
	θ (deg cm^2 dmol^{-1})	4860	1240	–900
(*S*,*S*)	λ max (nm)	291	448	526
	θ (mdeg)	–3.72	–0.7	1.13
	θ (deg cm^2 dmol^{-1})	–4430	–840	1340

to be associated with an electronic transition occurring within the Pd_3P_6 core ($d\sigma \rightarrow d\sigma^*$ type).[18] Knowing that the chiral ligands absorb only below 300 nm, the CD spectra indicate that the P-chirality is readily transposed to the Pd_3 core.

2 exhibits a chemically irreversible 2-electron reduction wave at ~ –0.65V *vs.* SCE (wave A_3; Fig. 3; $[Pd_3(dppm^*)_3(CO)(X)]^+ + 2e^- \rightarrow [Pd_3(dppm^*)_3(CO)]^0 + X^-$). During the anodic scan, the cyclic voltammogram (CV) exhibits two oxidation waves, A'_2 (–0.56) and A'_1 (–0.24 V *vs.* SCE). Such behavior has been previously observed by us for the achiral adducts of $[Pd_3(dppm)_3(CO)(X)]^+$ (X = halide or $CF_3CO_2^-$),[19] and a square scheme description (Scheme 4) for the observed CV traces is provided in Fig. 3 (A'_2; $[Pd_3(dppm)_3(CO)]^0$ (Pd_3^0) $\rightarrow [Pd_3(dppm)_3(CO)]^+$ ($Pd_3^{+\bullet}$) + 1e$^-$; A'_1; $[Pd_3(dppm)_3(CO)]^+$ ($Pd_3^{+\bullet}$) $\rightarrow [Pd_3(dppm)_3(CO)]^{2+}$ (Pd_3^{2+}) + 1e$^-$). The 2-electron reduction potential is associated with cluster **2**, but the $CF_3CO_2^-$ is located inside the cavity. Upon reduction, the guest anion escapes the cavity but does not re-enter inside it fast enough during the anodic sweep. So the species being oxidized are the corresponding neutral (Pd_3^0) and radical $Pd_3^{+\bullet}$ clusters. Of importance to the EPR study described below, the electrochemical findings indicate that the $Pd_3^{+\bullet}$ species exhibit empty cavities.

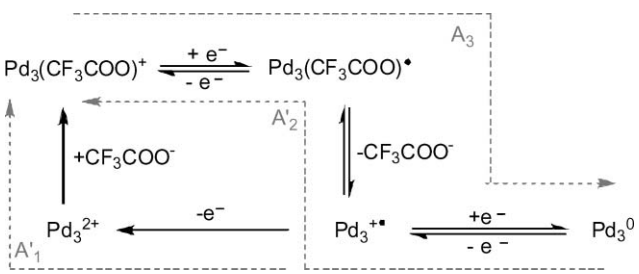

Scheme 4 Various processes taking place during the CV scans.

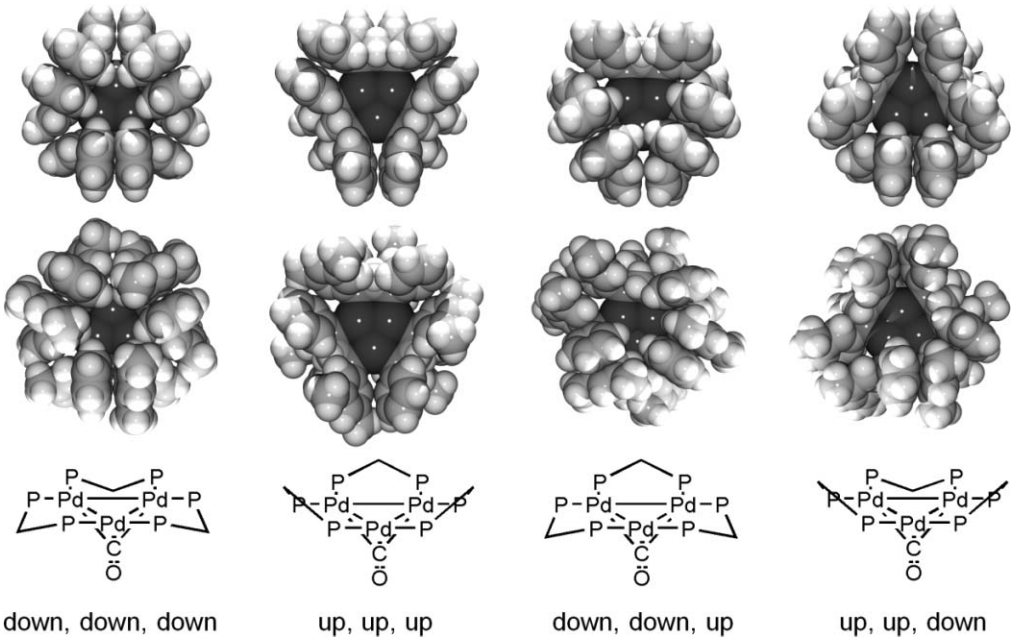

Fig. 1 Comparison of the cavity size above the Pd_3 plane for 4 possible conformations of the dppm ligands in $[Pd_3(dppm)_3(CO)]^{2+}$ (**2′**; first row) and dppm* ligands in $[Pd_3(dppm^*)_3(CO)]^{2+}$ (**2** ; second row). Up and down refer to the orientation of the PCH_2P chain with respect to the Pd_3 plane. The down, down, down conformation has never been observed.

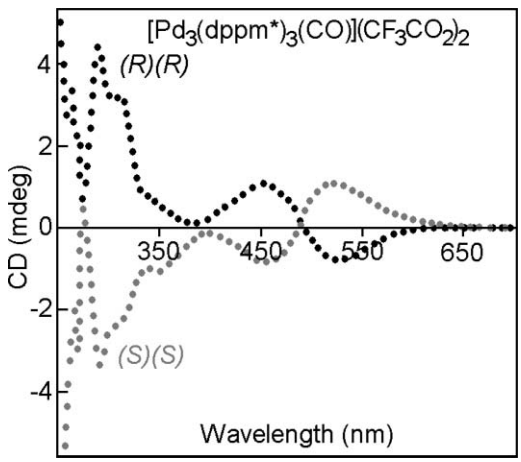

Fig. 2 CD spectra of **2** in THF at 298 K. dppm* = (*R*,*R*)- (black) and (*S*,*S*)-(*m*-XylPhP)$_2CH_2$, **1** (grey).

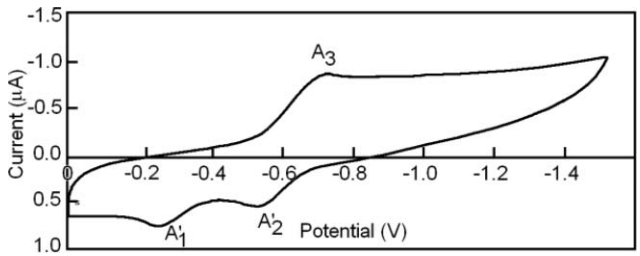

Fig. 3 CV of **2** in THF/Bu_4NPF_6. Starting potential = 0 V, scan rate = 0.1 V s^{-1}.

The bulk electrolysis of **2** at −1 V *vs.* SCE halted after transfer of one equivalent of electrons leads to $[Pd_3(dppm^*)_3(CO)]^{+\bullet}$ (**3**) (*via* the known dismutation reaction $[Pd_3(dppm^*)_3(CO)]^0$ + $[Pd_3(dppm^*)_3(CO)]^{2+} \rightarrow 2\ [Pd_3(dppm^*)_3(CO)]^{+\bullet}$) as unambiguously identified by the presence of the characteristic oxidation wave at −0.21 V (A'_1) and a reduction peak at −0.58 V.[7,8] This radical cation (**3**) is stable for several hours and has been characterized by EPR spectroscopy (Fig. 4).

The experimental EPR spectrum shown in Fig. 4A is strongly reminiscent of the symmetric septet previously reported for the $[Pd_3(dppm)_3(CO)]^{+\bullet}$ cluster (**3′**) (the EPR parameters of which are: $g = 2.065$, $A(^{31}P) = 75.8 \times 10^{-4}$ cm^{-1}, $A(^{105}Pd) = 7.6 \times 10^{-4}$ cm^{-1})[7] except that the five inner lines appear to be doubled. The origin of this effect can be explained by two slightly offset quartets, *i.e.* hyperfine splitting from *two sets of three* equivalent ^{31}P nuclei, as indicated by the successive "stick diagrams" shown in Fig. 4C. The observed spectrum covers a large field range (*ca.* 60 mT), and is strongly line-broadened at high field, leading to significant distortions from the ideal line intensities (Fig. 4A). This is attributed to tumbling insufficiently fast to average out the anisotropy of the hyperfine coupling tensor, an effect commonly seen for large radicals covering wide field/frequency ranges. Numerical fitting of the experimental spectrum (Fig. 4B), after correction for phase and baseline drift, using WinSim 0.98 software[20] converged to: $3 \times A(^{31}P) = 83.9 \times 10^{-4}$ cm^{-1}, $3 \times A(^{31}P) = 69.7 \times 10^{-4}$ cm^{-1}, $3 \times A(^{105}Pd) = 12.5 \times 10^{-4}$ cm^{-1}, LW = 5.5×10^{-4} cm^{-1}. A very good fit was obtained using purely Lorentzian lines and a line-width parameter of 7.9×10^{-4} cm^{-1}. The isotropic *g* value is 2.041. We think it is significant that the average $A(^{31}P)$ value of 76.8×10^{-4} cm^{-1} in the chiral $[Pd_3(dppm^*)_3(CO)]^{+\bullet}$ cluster (**3**) is *very* close to the 75.8×10^{-4} cm^{-1} observed in the achiral $[Pd_3(dppm)_3(CO)]^{+\bullet}$ (**3′**).[7] That three hyperfine coupling constants are significantly larger, and three smaller by a similar amount from the values in the achiral dppm cluster (**3′**), suggests that the *m*-xylyl groups induce a systematic change in conformation such

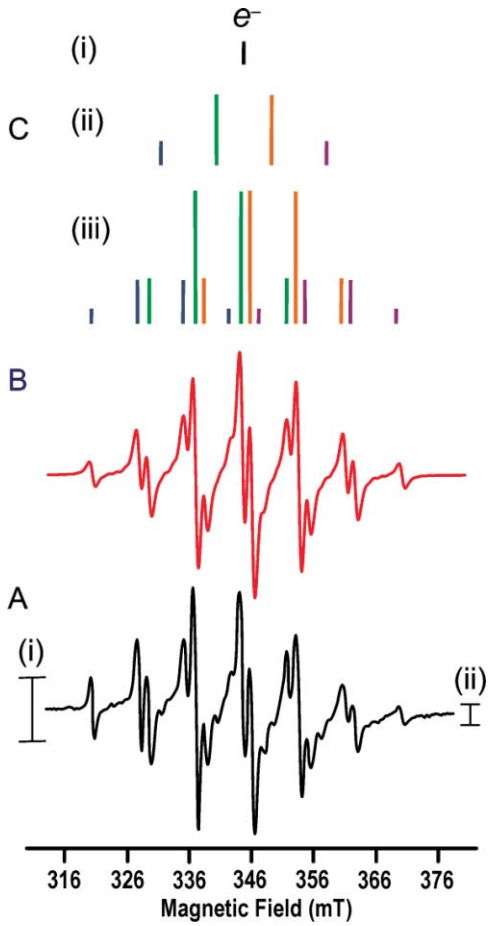

Fig. 4 Isotropic CW-EPR spectrum of the putative $[Pd_3(dppm^*)_3(CO)]^{+\bullet}$ radical cation (**3**) (dppm* = (*S*,*S*)-(*m*-XylPhP)$_2$CH$_2$) as measured at 298 K on extracts from the bulk electrolysis solution in THF. A) Experimental spectrum, with (i) low-field branch displaying 3 × intensity of (ii) the high-field branch. B) Line-fitted simulation calibrated to the average intensity. C) Interpretation of ^{31}P hfs: (i) free electron; (ii) 1 : 3 : 3 : 1 quartet from three equivalent P nuclei; (iii) each quartet in (ii) split further into 1 : 3 : 3 : 1 quartets by another three equivalent P nuclei (stick diagram in absorption mode).

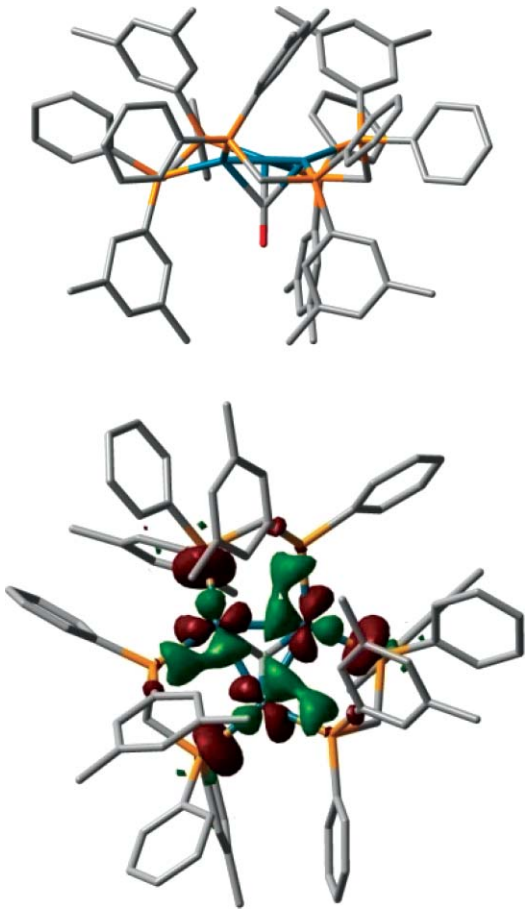

Fig. 5 $[Pd_3((S,S)\text{-dppm}^*)_3(CO)]^{+\bullet}$ radical cation (**3**); Top: side view of the optimized geometry. Bottom: representation of the SOMO.

that three ^{31}P nuclei *gain* in spin density, while the other three *lose* spin density compared to the achiral structure. We have previously observed in our studies of alkyne adducts of the achiral cluster (**3′**) that the sum of all six *A*(P) values remains remarkably stable even when the individual hyperfine coupling values differ greatly; spin density in these paramagnetic clusters remains strongly localized on the Pd_3P_6 core of the molecule.[9,10]

DFT computations were performed in order to examine the SOMO of the $[Pd_3((S,S)\text{-dppm}^*)_3(CO)]^{+\bullet}$ radical cation (**3**) (Fig. 5). First, its geometry was optimized, then the SOMO computed. This MO (Fig. 5, bottom) is composed of the Pd $d_{x^2-y^2}$ orbitals along the coordinating lone pairs of the P atoms, but importantly the shape of this MO exhibits distinctive C_3-symmetry. This C_3-induced distortion (compared to the expected C_{3v} point group of the achiral cluster (**3′**)) occurs because three of the phosphorus atoms are placed above the Pd_3 plane and three others are located below (Fig. 5, top). This distortion is most likely caused by the steric interactions among the xylyl groups since we do not find such distortions when similar calculations are performed on the achiral dppm cluster (**3′**).

Conclusions

We have prepared and characterized the first C_3-symmetry paramagnetic M-M-bonded clusters. This was achieved with the aid of new P-chirogenic diphosphines belonging to the dppm family. The C_3-symmetry was also confirmed by analyses of the EPR spectra wherein two sets of three chemically equivalent P atoms are detected. This conclusion is easily corroborated from DFT geometry optimizations where three P-atoms are found above the Pd_3 face, whereas the three others are below the face, by reference to the apical carbonyl. Consequently, the SOMO of the enantiomeric cluster has evident C_3-symmetry, such that the odd electrons are delocalised over Pd_3 metallic frames and placed in C_3-symmetry environment. This is unprecedented.

At the same time, we increased the stability of these highly reactive species relative to the achiral analogue $[Pd_3(dppm)_3(CO)]^{+\bullet}$ without using a capping RC≡CR ligand.[9,10] Consequently, the cluster cation radical lasts a long time while retaining reactivity and the C_3-symmetry cavity is available for substrate interactions.

Experimental

General

All reactions were carried out under an Ar atmosphere in dried glassware. Solvents were dried and freshly distilled under an Ar atmosphere over sodium/benzophenone for THF, diethylether, toluene and benzene and over CaH_2 for CH_2Cl_2. Hexane and isopropanol for HPLC were of chromatography grade and used without further purification. Methyllithium (1.6M in Et_2O), n-butyllithium (1.6M in hexanes), 5-bromo-*m*-xylene, $BH_3.SMe_2$, and 1,4-diazabicyclo[2.2.2]octane (DABCO) were purchased from Aldrich, Acros or Alfa Aesar, and used as received. (+)- and (−)-ephedrine were purchased from Aldrich and dried by azeotropic shift of toluene using a rotary evaporator. The toluenic HCl solution (0.2–0.4 M) was obtained by bubbling HCl gas in toluene and titrated by acidimetry before use. The (2*S*, 4*R*, 5*S*)-(−)- and its enantiomer (2*R*, 4*S*, 5*R*)-(+)-3,4-dimethyl-2,5-diphenyl-1,3,2-oxazaphospholidine-2-borane, were prepared from the appropriate (+)- or (−)-ephedrine, as previously described.[13] The (*Rp*)-(−)- and (*Sp*)-(+)-*N*-methyl-*N*-[(1-hydroxy-1-phenyl-prop-2-yl]aminophenyl-*m*-xylylphosphine borane were prepared according to the general procedure,[13] from (−)- or (+)-3,4-dimethyl-2,5-diphenyl-1,3,2-oxazaphospholidine-2-borane, respectively, and *m*-xylyl lithium reagent. Chiral HPLC analysis were performed on SHIMADZU 10-series apparatus, using chiral columns (Chiralcel OD–H, Chiralpack OJ), and with hexane/propan-2-ol mixtures as the mobile phase (Flow rate 1 mL min^{-1}; UV detection $\lambda = 254$ nm). Thin layer chromatography (TLC) was performed on 0.25 mm E. Merck precoated silica gel plates and exposed by UV, potassium permanganate or iodine treatment. Flash chromatography was performed with the indicated solvents using silica gel 60 A, (35–70 μm; Acros) or aluminium oxide 90 standardized (Merck). All NMR spectra data were recorded on BRUKER 300 AVANCE, 500 AVANCE DRX and 600 AVANCE II spectrometers at ambient temperature. Data are reported as *s* = singlet, *d* = doublet, *t* = triplet, *q* = quartet, *m* = multiplet, brs = broad singlet, brd = broad doublet, dhept = doublet of heptuplet, coupling constant(s) in Hertz. Melting points were measured on a Kofler bench melting point apparatus and are uncorrected. Optical rotations values were recorded at 20 °C on a Perkin-Elmer 341 polarimeter, using a 10 cm quartz vessel. Infrared spectra were recorded on a Bruker Vector 22 apparatus. Mass and HRMS spectra were recorded on Mass, Bruker ESI micro TOF-Q apparatus, at the Université de Bourgogne (Dijon). The major peak *m*/*z* was mentioned with the intensity as a percentage of the base peak in brackets. Elemental analyses were measured with a precision superior to 0.3% at the Microanalysis Laboratory of the Université de Bourgogne (EA 1108 CHNS–O FISONS Instrument).

Synthesis of the (*R*,*R*)- and (*S*,*S*)-(*m*-XylPhP)$_2$CH$_2$ ligands 1 (dppm*)

The (*R*,*R*)-ligand were prepared *via* its diborane complex, by reaction of the α-carbanion derived from the (*R*)-(−)-methylphenyl-*m*-xylylphosphine borane **6** with the (*S*)-chlorophenyl-*m*-xylylphosphine borane **5** , both prepared according to modified methodology starting from (+)-ephedrine,[13] The (*S*,*S*)-ligand **1** was prepared by a similar method starting from (−)-ephedrine.

(*Rp*)-(−)- or (*S*)-(+)-methylphenyl-*m*-xylylphosphine borane 6

The (*S*)-chlorophosphine **5** was obtained according to a general procedure outlined in ref. 13, and proceeds as follow. In a 50 mL two-necked flask equipped with a magnetic stirrer, an argon inlet and a rubber septum was introduced 2 mmol of (*Rp*)-(−)-*N*-methyl-[(1*R*,2*S*)(2-hydroxy-1-phenyl)ethyl]-aminophenyl-*m*-xylyl phosphine borane. A solution of HCl in toluene (0.38 M, 11.0 mL, 4.2 mmol, 2.1 equiv.) was next added under stirring at room temperature. After 1 h, the precipitate of ephedrine hydrochloride was filtered off with a Millipore 4 μm filter, and the excess HCl was removed by several vaccum/argon cycles. The toluene solution of chlorophosphine borane **5** obtained was used without further purification. Then, this solution was cooled at −78 °C and MeLi (0.87M, 5.7 mL, 5 mmol, 2.5 equiv.) was added. The reaction mixture was allowed to warm to RT during 1 h, and hydrolysed with water. The organic phase was removed and the aqueous layer was extracted with CH_2Cl_2, and the combined extracts were dried over $MgSO_4$, then concentrated. The residue was purified by chromatography on a short column of silica gel with toluene/petroleum ether: 7/3 as eluent, to give the methylphenyl-*m*-xylylphosphine borane **6**. It was recrystallized in a mixture of isopropyl alcohol/hexane, affording enantiomerically pure phosphine borane as white needle crystals. The enantiomeric purity was checked by HPLC (Chiralcel OJ, Hexane/iPrOH 90 : 10, 1 mL min^{-1}, $\lambda = 254$ nm, t_R (*R*) = 11.1 min, t_R (*S*) = 14.8 min). Yield = 99%; colorless oil; $[\alpha]_D^{25} = -9.9$ ($c = 0.6$, $CHCl_3$) for e.e. > 99%; R_f 0.70 (toluene); IR (KBr, ν/cm^{-1} 3074-2852 (C–H), 2380 (B–H), 1604, 1548, 1459, 1271, 1134, 825, 735; ^{1}H NMR ($CDCl_3$) δ (ppm) 0.56–1.48 (q, 3H, $^3J_{BH} = 96$, BH_3), 1.86 (d, 3H, $^2J_{PH} = 10.2$, P–CH_3), 2.35 (s, 3H,CH_3), 7.14 (br, 1H, *H* arom), 7.29 (d, 2H, $J = 11.1$, *H* arom.), 7.42–7.54 (m, 3H, *H* arom), 7.65–7.81 (m, 2H, *H* arom.); ^{13}C NMR ($CDCl_3$) δ (ppm) 11.9 (d, $^1J_{PC} = 40.2$, P–*C*H$_3$), 21.3 (*C*H$_3$), 128.8 (d, $J_{PC} = 10.5$, *C* arom.), 129.3 (d, $J_{PC} = 9.7$, *C* arom.), 130.4 (d, $J_{PC} = 22.5$, *C*q arom.), 131.0 (d, $J_{PC} = 2.6$, *C* arom.), 131.7 (d, $J_{PC} = 9.7$, *C* arom.), 133 (d, $J_{PC} = 2.6$, *C* arom.), 138.5 (d, $J_{PC} = 10.5$, *C*q arom.); ^{31}P NMR ($CDCl_3$) δ (ppm) +9.4 (q, $^1J_{PB} = 68.9$); MS (EI) *m*/*z* (relative intensity) 265 (M^+ + Na, 100), 281 (18); HRESI-MS (CH_2Cl_2) calcd for $C_{15}H_{20}BNaP$ [M+Na^+]: 265.1288; found: 265.1278; Anal. Calcd for $C_{15}H_{20}BP$ (242.109): C 74.41, H 8.33; found: C 74.04, H 8.34.

The (*S*)-(+)-methylphenyl-*m*-xylylphosphine borane **6** , which was prepared from the (+)-3,4-dimethyl-2,5-diphenyl-1,3,2-oxazaphospholidine-2-borane derived from (−)-ephedrine, exhibits satisfactory analytical data in agreement with the (*R*)-(−)-enantiomer.

Preparation of the (*R*,*R*)-(+)- or (*S*,*S*)-(−)-bis(phenyl-*m*-xylylphosphino borane)methane 7 (dppm*)

A 100 mL two-necked flask equipped with a magnetic stirrer, an argon inlet and a rubber septum was charged with 1.08 g of the (*R*)-(−)-phosphine borane **6** (4.40 mmol, 3 equiv.) in 10 mL of THF, and cooled to 0 °C. 2.8 mL of *n*-BuLi (1.6 M in hexane, 4.40 mmol, 3 equiv.) was added dropwise. The reaction was maintained at this temperature for 30 min, then the cooling bath was removed and the reaction stirred at room temperature for 90 min. After cooling at −78 °C, a

freshly prepared toluene solution of the chlorophosphine borane **5** (1.47 mmol, 1 equiv.) from (*Rp*)-(−)-*N*-methyl-[(1*R*,2*S*)(2-hydroxy-1-phenyl)ethyl]-aminophenyl-*m*-xylyl phosphine borane, was then added dropwise under stirring to the anion solution. The mixture was slowly warmed room temperature overnight. After hydrolysis, the aqueous layer was extracted with 3 × 30 mL of CH_2Cl_2, and the combined extracts were dried over $MgSO_4$, then concentrated. The residue was purified by chromatography on a short column of silica gel with toluene as eluent, to give the diphosphine as diborane complex. It was recrystallized in CH_2Cl_2, by slow diffusion of heptane, affording diastereomerically and enantiomerically pure white needle crystals. The diastereomeric and enantiomeric purity of the diphosphine diborane **7** was controlled by HPLC analysis on a Chiralcel OD–H Daicel column, eluent: hexane/i-PrOH 98 : 2, 0.25 mL min^{-1}, $\lambda = 254$ nm; (*R*,*R*), $t_R = 35$ min; (*S*,*S*)-enantiomer $t_R = 37$ min; (*R*,*S*), $t_R = 26$ min.

Yield = 70%; mp = 154 °C; R_f 0.1 (toluene: petroleum ether/1 : 1); $[\alpha]_D^{20} = +26$ (c 0.5, $CHCl_3$) for 99% e.e.; IR (solid) (cm^{-1}) 3057–2860, 2384, 1437, 1136, 1060. ^{1}H NMR ($CDCl_3$) δ (ppm) 0.75–1.15 (6H, m, $^1J_{BH} = 116$, BH_3), 2.17 (6H, s, CH_3), 3.14 (2H, t, $^2J_{PH} = 10.8$, CH_2), 6.83 (2H, s, Ar), 7.11 (6H, d, $^3J_{HH} = 12$, Ar), 7.39–7.23 (6H, m, Ar), 7.61–7.48 (4H, m, Ar); ^{13}C NMR ($CDCl_3$) δ (ppm): 21.2 (CH_3), 23.6 (t, $J_{PC} = 26$, CH_2), 127.0 (d, $J_{PC} = 61$, C_q), 128.6 (d, $J_{PC} = 10$, C_{arom}), 129.5 (s, C_q), 130.3 (d, $J_{PC} = 10$, C_{arom}), 131.2 (d, $J_{PC} = 2$, C_{arom}), 132.4 (d, $J_{PC} = 10$, C_{arom}), 133.2 (d, $J_{PC} = 2$, C_{arom}), 138.1 (d, $^1J_{PC} = 11$, C_q); ^{31}P NMR ($CDCl_3$) δ (ppm): +14,4 (m). HRESI-MS (CH_2Cl_2) calcd for $C_{29}H_{36}B_2NaP_2$ [M+Na$^+$]: 491.2371; found: 491.2362. Anal. calcd (%) for $C_{29}H_{36}B_2P_2$: C 74.36, H 7.69; found: C 74.11, H 8.15.

The (*S*,*S*)-(−)-**7** which was prepared from the (*S*)-(+)-methylphenyl-*m*-xylylphosphine borane **6** derived from (−)-ephedrine, exhibits satisfactory analytical data in agreement with the (*R*,*R*)-(+)-enantiomer. The *meso*-isomer (*R*,*S*)-**1** was prepared by reaction of the α-carbanion derived from the (*R*)-(−)-methylphenyl-*m*-xylylphosphine borane **6** with the (*R*)-chlorophenyl-*m*-xylylphosphine borane **5** obtained using the (−)-ephedrine pathway.

(*R*,*R*)-(−)- or (*S*,*S*)-(+)bis(phenyl-*m*-xylylphosphino)methane 1

The (*R*,*R*)-diphosphine diborane **7** (0.11 mmol) was placed in a three-necked flask fitted with a reflux condenser, a magnetic stirrer, and an argon inlet. A solution of DABCO (0.44 mmol) in toluene (4 mL) was added, and the flask was purged three times with argon. The mixture was heated to 50 °C for 12h and the crude product was rapidly purified on a short column of neutral alumina (15 cm height, 2 cm diameter) using a degassed toluene–AcOEt (9 : 1) mixture as eluent. After removal of the solvent, the free ligand **1** was obtained quantitatively and used without further purification. R_f 0.87 (toluene; CCM neutral alumina); $[\alpha]_D^{20} = -3.0$ (c 0.5, $CHCl_3$); ^{1}H NMR ($CDCl_3$) δ (ppm): 2.21 (12H, s, CH_3), 2.70 (2H, t, $J = 1.0$, CH_2), 6.84 (2H, s, Ar), 6.96–6.94 (4H, t, $J = 3.3$, Ar), 7.22–7.18 (6H, m, Ar), 7.39–7.32 (4H, m, Ar). ^{13}C NMR ($CDCl_3$) δ (ppm): 21.3 (s, CH_3), 27.8 (t, $J_{PC} = 2.3$, CH_2), 77.2 (C_{arom}), 128.2 (t, $J_{PC} = 3.3$, C_{arom}), 128.5 (s, C_{arom}), 130.6 (t, $J_{PC} = 10.0$, C_{arom}), 132.8 (t, $J_{PC} = 10.0$, C_{arom}), 137.7 (t, $J_{PC} = 3.8$, C_q), 138.2 (t, $J_{PC} = 2.7$, C_q), 139.2 (t, $J_{PC} = 3.9$, C_q); ^{31}P NMR ($CDCl_3$) δ (ppm): −22.5 (s). HRESI-MS (CH_2Cl_2) calcd for $C_{29}H_{30}NaP_2$ [M+Na$^+$]: 463.1715; found: 463.1691.

The (*S*,*S*)-(+)-**1** which was obtained from the (*S*,*S*)-(−)-bis(phenyl-*m*-xylylphosphino borane)methane **7** , exhibits satisfactory analytical data in agreement with the (*R*,*R*)-(−)-enantiomer.

Synthesis of $[Pd_3(dppm^*)_3(CO)](CF_3CO_2)_2$ 2 (dppm* = (*R*,*R*)- or (*S*,*S*)-(*m*-XylPhP)$_2CH_2$ 1)

A 100 mL two-necked flask equipped with a magnetic stirrer, an argon inlet and a rubber septum was charged with (*R*,*R*)- or (*S*,*S*)-(*m*-XylPhP)$_2CH_2$ **1** (51.5 mg, 0.116 mmol) and $Pd(OAc)_2$ (25.4 mg, 0.113 mmol) in acetone (7 mL), trifluoroacetic acid (1.5 mL), and H_2O (1 mL). The mixture was transferred into an autoclave and was allowed to react under CO pressure (700 psi) for 16 h. The solvent was removed under vacuum after filtration, and the resultant dark red oil was extracted with toluene several times. After filtration, the solvent of the red solution was removed under vacuum. Yield 40% (53 mg), mp= 100 °C (decomp.). IR (solid) (ν/cm^{-1}: 3065–2867, 1814, 1687, 1436, 1196, 1140, 743. ^{1}H NMR ($CDCl_3$) δ :7.79–7.27 (m, 6H, Ar), 7.80 (br, 16H, Ar), 7.18–6.92 (m, 18H, Ar), 6.72 (br, 4H, Ar), 6.66 (br, 2H, Ar), 6.56 (br, 2H, Ar), 4.71 (br, 2H, CH_2), 4.11 (br, 2H, CH_2), 2.96 (br, 2H, CH_2), 2.35 (br, 6H, CH_3), 2.28–2.17 (m, 9H, CH_3), 2.03 (br, 6H, CH_3), 1.98 (br, 6H, CH_3), 1.25 (br, 6H, CH_3), 0.88 (br, 3H, CH_3). ^{13}C NMR ($CDCl_3$) δ: 137.9 (*C*O), 132.9 (C_{arom}), 132,0 (C_{arom}), 130.8 (C_{arom}), 129.6 (C_{arom}), 129.0 (C_{arom}), 128.2 (C_{arom}), 127.8 (C_{arom}), 125.3 (C_{arom}), 29.7 (CH_2), 21.4 (CH_3), 20.9 (CH_3). ^{31}P NMR ($CDCl_3$) δ: −9.1 (s). ESI *m*/*z* (relative intensity): 1703.22 ([$C_{88}H_{90}P_6Pd_3$ + Cl]$^+$, 100). HRESI-MS (CH_2Cl_2) calcd for [$C_{88}H_{90}Cl_1O_1P_6Pd_3$]: 1701.2205; found: 1701.2224, calcd for [$C_{90}H_{90}F_3O_3P_6Pd_3$]: 1779.2367; found: 1779.2424. Anal. calcd for $C_{92}H_{90}F_6O_5P_6Pd_3$: C 58.35, H 4.76; O 4.23 found: C 58.02, H 5.04, O 3.98.

Electrochemical experiments

All manipulations were performed using Schlenk techniques in an atmosphere of dry oxygen-free argon. The supporting electrolyte, ^{n}Bu$_4$NPF$_6$, was degassed under vacuum before use and then dissolved to a concentration of 0.2 mol L^{-1}. For cyclic voltammetry experiments, the concentration of the analyte was almost 10^{-3} mol L^{-1}. Voltammetric analyses were carried out in a standard three electrode cell using an EG&G Princeton Applied Research (PAR) Model 263A potentiostat, interfaced to a computer running Electrochemistry Power Suite software. The reference electrode was a saturated calomel electrode (SCE) separated from the solution by a sintered glass disk. The auxiliary electrode was a platinum wire. For all voltammetric measurements, the working electrode was a vitreous carbon disk (nominal diameter = 3 mm). Under these conditions, when operating in THF, the formal potential for the ferrocene (+/0) couple was found to be +0.56 V *versus* the SCE. Controlled potential electrolysis was performed with an Amel 552 potentiostat coupled with an Amel 721 electronic integrator. Bulk electrolyses were performed in a cell with three compartments separated with glass frits of medium porosity. Carbon gauze was used as the working electrode, a platinum plate as the counter-electrode and a saturated calomel electrode as the reference electrode.

Computations. DFT

The electronic structure optimizations were calculated with Gaussian 03,[21] at the Université de Sherbrooke's Mammouth super computer, supported by the Réseau Québécois de Calcul de Haute Performance. The DFT[22–25] was calculated by the B3LYP[26–28] method with specific basis sets assigned for different atom types. For C, H, O and P, all the electrons were described by 3-21G*[29–34] basis set; Palladium was described by SBKJC VDZ[29,35–39] and Stuttgart-Koeln MCDHF RSC ECP.[40–43]

Circular dichroism spectra

Circular dichroism measurements were performed on a Jasco J-810 spectropolarimeter equipped with a Jasco Peltier-type thermostat. The instrument was calibrated with an aqueous solution of (+)-10-camphorsulfonic acid at 290.5 nm. Samples were loaded into quartz cells with a path length of 0.1 cm. Far-UV CD spectra were recorded at the desired temperature from 190 to 700 nm by averaging three scans at 0.1 nm intervals.

EPR spectrum and simulation

EPR spectra were acquired on a BRUKER Elexsys E500 spectrometer in CW mode. The experimental spectrum selected for line-fitting was corrected for baseline drift, but remains significantly line broadened at high field due to slow tumbling. The simulation was obtained using Lorentzian lines with WinSim 0.98 (Public EPR Software Tools, NIEHS) with full line-shape fitting. The spectrum features coupling to two sets of three equivalent ^{31}P nuclei; additional weak features result from satellites from coupling to three equal ^{105}Pd nuclei (22% abundant).

Computer modelling

The space filling models used in Fig. 1 were computed using PCModel version 7.0 software from Serena Software.

Acknowledgements

PDH thanks the Natural Sciences and Engineering Research Council of Canada (NSERC), Fonds Québécois de la Recherche sur la Nature et la Technologie, and Centre d'Etudes des Matériaux Optiques et Photoniques de l'Université de Sherbrooke for funding and Dr P. Lavigne from the Faculté de Médecine of the Université de Sherbrooke for use of his circular dichroism spectrometer. SJ acknowledges Pr. C. Darcel for fruitful discussions on ligand synthesis and Ms. M. J. Penouilh (Centre de Spectroscopie, Dijon), for NMR analysis and mass spectroscopy. RTB thanks NSERC for ongoing support.

References

1 M. P. Sibi, S. Manyem, S. Zimmerman and J. Zimmerman, *Chem. Rev.*, 2003, **103**, 3263.
2 A. Sarkar and S. Pal, *Eur. J. Inorg. Chem.*, 2009, 622.
3 A. Gonzalez-Alvarez, I. Alfonso, J. Cano, P. Diaz, V. Gotor, V. Gotor-Fernandez, E. Garcia-Espana, S. Garcia-Granda, H. Jimenez and F. Lloret, *Angew. Chem., Int. Ed.*, 2009, **48**, 6055.
4 L. Lisnard, P. Mialane, A. Dolbecq, J. Marrot, M. J. Clemente-Juan, E. Coronado, B. Keita, P. de Oliveira, L. Nadjo and F. Secheresse, *Chem. Eur. J.*, 2007, **13**, 3525; F. Lin-Lin, G. Fu-Sheng, Y. Lei, L. Zhuo-Jia, H. Radovan, L. Ji-Dong, O. Yong-Cong and T. Ming-Liang, *Dalton Trans.*, 2010, **39**, 1771; S.-M. Hu, S.-C. Xiang, J.-J. Zhang, T.-L. Sheng, R.-B. Fu and X.-T. Wu, *Eur. J. Inorg. Chem.*, 2008, **7**, 1141; A. Burkhardt, E. T. Spielberg, H. Görls and W. Plass, *Inorg. Chem.*, 2008, **47**, 2485; Y. Li, S. Xiang, T. Sheng, J. Zhang, S. Hu, R. Fu, X. Huang and X. Wu, *Inorg. Chem.*, 2006, **45**, 6577; M.-L. Fu, G.-C. Guo, A.-Q. Wu, B. Liu, L.-Z. Cai and J.-S. Huang, *Eur. J. Inorg. Chem.*, 2005, 3104; C.-M. Liu, R.-G. Xiong, D.-Q. Zhang and D.-B. Zhu, *J. Am. Chem. Soc.*, 2010, **132**, 4044.
5 U. Honrath and H. Vahrenkamp, *Z. Naturforsch., B: Anorg. Chem., Org. Chem.*, 1984, **39B**, 559.
6 A. Benoit, A. Darchen, J. Y. Le Marouille, C. Mahé and H. Patin, *Organometallics*, 1983, **2**, 555.
7 D. Brevet, D. Lucas, H. Cattey, F. Lemaître, Y. Mugnier and P. D. Harvey, *J. Am. Chem. Soc.*, 2001, **123**, 4340.
8 F. Lemaître, D. Lucas, K. Groison, P. Richard, Y. Mugnier and P. D. Harvey, *J. Am. Chem. Soc.*, 2003, **125**, 5511.
9 S. Dal Molin, C. Cugnet, D. Brevet, D. Lucas, Y. Mugnier, D. Fortin, R. T. Boeré and P. D. Harvey, *Organometallics*, 2007, **26**, 5209.
10 C. Cugnet, S. Dal Molin, D. Brevet, D. Lucas, Y. Mugnier, P. D. Harvey and R. T. Boeré, *Can. J. Chem.*, 2009, **87**, 103.
11 C. Salomon, D. Fortin, C. Darcel, S. Jugé and P. D. Harvey, *J. Cluster Sci.*, 2009, **20**, 267.
12 S. Jugé, J. P. Genêt, J. A. Laffitte, M. Stéphan, Fr. Patent 91 01674 (1991); S. Jugé, R. Merdès, M. Stéphan and J.-P. Genêt, *Phosphorus and Sulfur* 1993, 77, 199; C. Darcel, J. Uziel and S. Jugé, in *Phosphorus Ligands in Asymmetric Catalysis Synthesis and Applications*, A. Börner (ed.), 2008, Wiley-VCH.
13 C. Bauduin, D. Moulin, E. B. Kaloun, C. Darcel and S. Jugé, *J. Org. Chem.*, 2003, **68**, 4293.
14 B. R. Lloyd and R. J. Puddephatt, *Inorg. Chim. Acta*, 1984, **90**, L77.
15 L. Manojlovic-Muir, K. W. Muir, B. R. Lloyd and R. J. Puddephatt, *J. Chem. Soc., Chem. Commun.*, 1985, 536.
16 L. Manojlovic-Muir, K. W. Muir, B. R. Lloyd and R. J. Puddephatt, *J. Chem. Soc., Chem. Commun.*, 1983, 1336.
17 R. Provencher, K. T. Aye, M. Drouin, J. Gagnon, N Boudreault and P. D. Harvey, *Inorg. Chem.*, 1994, **33**, 3689.
18 P. D. Harvey, S. Hubig and T. Ziegler, *Inorg. Chem.*, 1994, **33**, 3700.
19 I. Gauthron, Y. Mugnier, K. Hierso and P. D. Harvey, *Can. J. Chem.*, 1997, **75**, 1182; F. Lemaître, D. Lucas, D. Brevet, A. Vallat, P. D. Harvey and Y. Mugnier, *Inorg. Chem.*, 2002, **41**, 2368.
20 WinSim (v.0.98, 2002) software: D. R. Duling, *J. Magn. Reson.*, 1994, **B104**, 105.
21 M. J. Frisch, G. W. Trucks, H. B. Schlegel, G. E. Scuseria, M. A. Robb, J. R. Cheeseman, V. G. Zakrzewski, J. A. Jr. Montgomery, R. E. Stratmann, J. C. Burant, S. Dapprich, J. M. Millam, A. D. Daniels, K. N. Kudin, M. C. Strain, O. Farkas, J. Tomasi, V. Barone, M. Cossi, R. Cammi, B. Mennucci, C. Pomelli, C. Adamo, S. Clifford, J. Ochterski, G. A. Petersson, P. Y. Ayala, Q. Cui, K. Morokuma, D. K. Malick, A. D. Rabuck, K. Raghavachari, J. B. Foresman, J. Cioslowski, J. V. Ortiz, A. G. Baboul, B. B. Stefanov, G. Liu, A. Liashenko, P. Piskorz, I. Komaromi, R. Gomperts, R. L. Martin, D. J. Fox, T. Keith, M. A. Al-Laham, C. Y. Peng, A. Nanayakkara, C. Gonzalez, M. Challacombe, P. M. W. Gill, B. G. Johnson, W. Chen, M. W. Wong, J. L. Andres, M. Head-Gordon, E. S. Replogle and J. A. Pople, *Gaussian 98* (Revision A.6), Gaussian, Inc., Pittsburgh PA, 1998.
22 P. Hohenberg and W. Kohn, *Phys. Rev.*, 1964, **136**, B864.
23 W. Kohn and L. J. Sham, *Phys. Rev.*, 1965, **140**, A1133.
24 *The Challenge of d and f Electrons*, ed. D. R. Salahub, M. C. Zerner, ACS, Washington, D.C., 1989.
25 R. G. Parr and W. Yang, *Density-functional theory of atoms and molecules*, Oxford Univ. Press, Oxford, 1989.
26 A. D. Becke, *J. Chem. Phys.*, 1993, **98**, 5648.
27 C. Lee, W. Yang and R. G. Parr, *Phys. Rev. B: Condens. Matter Mater. Phys.*, 1988, **37**, 785.
28 B. Miehlich, A. Savin, H. Stoll and H. Preuss, *Chem. Phys. Lett.*, 1989, **157**, 200.
29 J. S. Binkley, J. A. Pople and W. J. Hehre, *J. Am. Chem. Soc.*, 1980, **102**, 939.
30 M. S. Gordon, J. S. Binkley, J. A. Pople, W. J. Pietro and W. J. Hehre, *J. Am. Chem. Soc.*, 1982, **104**, 2797.
31 W. J. Pietro, M. M. Francl, W. J. Hehre, D. J. Defrees, J. A. Pople and J. S. Binkley, *J. Am. Chem. Soc.*, 1982, **104**, 5039.
32 K. D. Dobbs and W. J. Hehre, *J. Comp. Chem.*, 1986, **7**, 359.
33 K. D. Dobbs and W. J. Hehre, *J. Comp. Chem.*, 1987, **8**, 861.
34 K. D. Dobbs and W. J. Hehre, *J. Comp. Chem.*, 1987, **8**, 880.

35 Basis Set Exchange Library https://bse.pnl.gov/bse/portal.
36 W. J. Stevens, H. Basch and M. Krauss, *J. Chem. Phys.*, 1984, **81**, 6026.
37 W. J. Stevens, M. Krauss, H. Basch and P. G. Jasien, *Can. J. Chem.*, 1992, **70**, 612.
38 T. R. Cundari and W. J. Stevens, *J. Chem. Phys.*, 1993, **98**, 5555.
39 Stuttgart-Koeln MCDHF RSC ECP EMSL Basis Set Exchange Library https://bse.pnl.gov/bse/portal.
40 D. Figgen, G. Rauhut, M. Dolg and H. Stoll, *Chem. Phys.*, 2005, **311**, 227.
41 K. A. Peterson, D. Figgen, M. Dolg and H. Stoll, *J. Chem. Phys.*, 2007, **126**, 124101.
42 B. C. Shepler, D. Figgen and H. Stoll, *J. Phys. Chem. A*, 2006, **110**, 13877.
43 D. Figgen, K. A. Peterson, M. Dolg and H. Stoll, *J. Chem. Phys.*, 2009, **130**, 164108.